ANALES DE MECANICA DE LA FRACTURA VOL. 16 (1999)

CYCLIC STRESS-STRAIN FIELDS IN THE VICINITY OF A CRACK TIP IN A STRAIN-HARDENING MATERIAL

V. Kharin and J. Toribio

Universidad de La Coruña (ULC)
Departamento de Ciencia de Materiales
ETSI Caminos, Campus de Elviña, 15071 La Coruña, Spain

Abstract.– Finite-element large-deformation analysis of the cracked strain-hardening elastoplastic solid under cyclic loading was performed. Minor quantitative changes, but not essential distinctions, were found in the near tip stress fields comparing the data corresponding to different hardening rules (isotropic, kinematic and combined) with the perfectly-plastic constitutive model (with no strain hardening). With regard to the deformations, strain-hardening promotes formation of localised slip bands in the fatigue crack tip. This affects the strain field shape and the rates of plastic strain accumulation in certain locations. The implications of the simulation results for criteria of fatigue damage accumulation are discussed focusing on the role of loading regime (amplitude and overloads) on the fatigue crack propagation rate.

Resumen.– Se ha realizado un análisis por elementos finitos, en grandes deformaciones, del sólido elastoplástico fisurado, con capacidad de endurecimiento por deformación, sometido a carga cíclica. Sólo se detectaron pequeñas diferencias, mas no cambios esenciales, en los campos tensionales próximos al extremo de la fisura obtenidos utilizando diferentes tipos de endurecimiento (cinemático, isótropo y combinado), al compararlos con el modelo constitutivo perfectamente plástico (sin endurecimiento por deformación). Con respecto a las deformaciones, el endurecimiento por deformación potencia la formación de bandas de deslizamiento localizadas en el extremo de la fisura de fatiga. Esto afecta a la forma del campo tensional y a la tasa de acumulación de deformación plástica en determinados lugares. Las implicaciones de los resultados en cuanto a criterios de acumulación de daño por fatiga se discuten en lo relativo al papel del régimen de carga (amplitud y sobrecargas) en la tasa de crecimiento de fisuras por fatiga.

1. INTRODUCTION

Analyses of the crack tip stress and deformation fields are essential for understanding of the crack propagation phenomena and for development of the predictive tools by means of linking relevant stress-strain characteristics to microscopical rupture mechanisms. Extensive studies of the elastoplastic near-tip fields under fatigue have been accomplished within the small-deformations approach for a variety of material constitutive equations, see e.g. [1-5]. Advanced high-resolution studies of the crack tip fields have also been performed taking into account both constitutive (plasticity) and geometrical (large deformations) nonlinearities which are equally essential to gain realistic implications for fracture [6,7]. However, only the monotonic loading situations have received exhaustive consideration there. In relation to fatigue, a thorough study accounting for the roles of plasticity and large geometry changes has been performed dealing with the perfectly-plastic solid [8,9]. Only quite limited data have been generated till now considering real materials under cyclic loading [10,11].

This contribution focuses on the effect of the strain-hardening constitutive behaviour on the near-tip situation under cyclic loading to provide more insight about fatigue cracking. Finite deformation simulations of the crack tip fields in the strain-hardening elastoplastic solid were performed for a plane-strain crack subjected to mode I (opening) cyclic loading under small scale yielding. The latter allows to use the linear elastic fracture mechanics tool —the stress intensity factor K— as the controlling parameter of the elastoplastic crack tip situation irrespective of the geometry of a solid and distribution of applied loads.

2. DESIGN OF THIS STUDY

The model of perfectly-plastic solid, although it is quite suitable for analytical and numerical evaluations, does not accurately represent the constitutive response of materials which usually manifest strain hardening. It may be useful to improve the approximation adopting as the controlling material parameter not simply a conventional engineering yield strength $\sigma_{0.2}$, but a suitable effective value of the yield stress σ_Y as modified by strain hardening. Then, owing to the similitude of the corresponding elastoplastic solutions with respect to σ_Y and the dimensionless factor σ_Y/E, where E is the Young modulus, strain hardening of materials may affect only the scaling of stress-strain fields, but not their shape, under otherwise similar geometry-and-loading circumstances, e.g. near cracks.

It is clear that "irrespective of the method of solution, the results of an elastic-plastic analysis are as good as the constitutive model employed" [5]. While certain model deficiencies may not substantially alter results in many analysis tasks, usually it is not easy to perceive *a priori* if a model in use would not miss important features of the stress-strain fields in question. In relation to the crack tip fields, it seems to be useful to consider various constitutive models focusing on their possible effects on the crack tip situation in fatigue.

As a model, the rate-independent strain-hardening elastoplastic material with von Mises yield surface was considered. The monotonic loading characteristics of the material corresponded to the experimental data for a cold-drawn high-strength steel [12] as follows: E = 195 GPa, Poisson ratio μ = 0.3, the value of 0.2% offset yield strength taken as the initial tensile yield stress σ_Y = 1500 MPa. The monotonic stress-strain curve of the steel is approximated by the Ramberg-Osgood equation which relates the plastic component of the total equivalent strain ε_{eq}^p to the equivalent stress σ_{eq} as

$$\varepsilon_{eq}^p = (\sigma_{eq}/P)^n \qquad (1)$$

where the strain hardening exponent and the strength coefficient respectively are n = 17 and P = 2160 MPa.

The basic approaches to handle strain-hardening are the isotropic and kinematic hardening models, as well as the combined isotropic-to-kinematic hardening rule. Although they are known to be quite limited with regard to the ability to rationalise typical phenomena of cyclic plasticity [13], such as cyclic softening, ratcheting, etc., they were chosen as the first step to elucidate various aspects of cyclic plastic deformation near the crack tip with account for strain hardening. The case of perfect plasticity was also considered for comparisons.

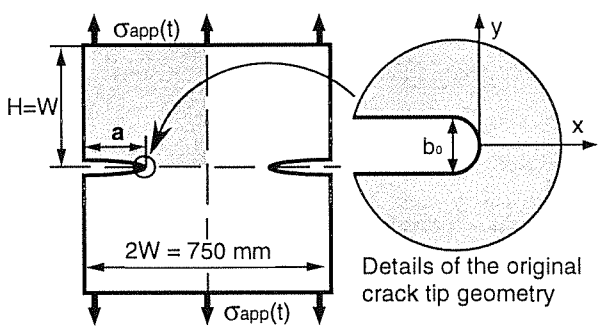

Fig. 1. The model testpiece geometry and applied load.

Confining to K-controlled small-scale yielding situation, model geometry and loading were taken the same as in the previous simulations for the case of perfect plasticity [8,9]. The double-edge-cracked panel under remote tension by applied stresses σ_{app} was considered (Fig. 1). The undeformed crack has parallel flanks and smooth round-shape tip of the width (twice the radius) b_0 = 5 μm.

On the basis of the experiments with the prototype steel [12], the following fatigue regimes in relation to its fracture toughness K_{IC} = 84 MPa·m$^{1/2}$ were chosen:

(I) $K_{max} = 0.6K_{IC}$;
(II) $K_{max} = 0.8K_{IC}$;
(III) $K_{max} = 0.6K_{IC}$, $K_{ov} = 0.85K_{IC}$ in the 4th cycle

(always K_{min} = 0), where K_{max} and K_{min} are respectively the maximum and minimum K-levels at constant amplitude cycling; K_{ov} corresponds to an overload peak.

The finite-element code MARC [14] was employed with updated Lagrangian formulation to perform an elastoplastic analysis with large displacements and large strains. Owing to the symmetry, simulations were carried out for the one-quarter of the panel (shadowed on the testpiece scheme in Fig. 1). To avoid premature degeneration of the finite-element mesh and to allow completion of several load reversals, the near tip mesh and the load stepping procedure in the incremental elastoplastic solution had to be finer than in similar studies of monotonic loading or a perfectly-plastic material [6-10]. Various meshes of four-node quadrilateral finite elements were tried. For the perfectly plastic case the fairly sufficient mesh had 1148 elements with 1222 nodes with the average size of the smallest elements adjacent to the tip of $0.046b_0$ [8,9]. To succeed in dealing with strain hardening effects required the finer mesh of 2189 elements and 2284 nodes with the smallest element mean dimension $0.016b_0$. The number of load steps between load extremes was set typically at 200, but in some trials the number was taken to be as high as 400. Prescribed loading routes consisted typically of up to ten cycles.

3. RESULTS

Under coarse examination, cyclic crack tip fields at all kinds of hardening rule display affinity between each other and with perfectly-plastic material behaviour, this latter being essentially the same as described elsewhere [8,9]. However, at higher resolution, strain hardening seems to be the promoter of substantial fine-scale distinctions which are clearly raised by progressing accumulation of plastic strain.

3.1. Crack Tip Deformations

The crack tip profiles evolve with load cycling in a similar manner for all considered strain-hardening rules and loading regimes. At the initial stages of loading, the tip shapes remain smooth like those observed in a perfectly-plastic solid [8,9]. However, whilst loading continues, the smoothly curved tip flattens out and acquires a cornered shape, as shown in Fig. 2. This is accompanied by the development of shear bands from the corners and appearance of the wedge-shaped region in front of the tip apex which undergoes little deformation since then. The point in the crack plane where one of

these bands intersects with its symmetric counterpart is also the location of the internal peak of plastic strain accumulation. With the same kind of strain-hardening, the higher level of the applied load (K_{max} or K_{ov}) which has been ever attained, the lower the number of cycles N for which cornering and strain localisation start. In the matter of the hardening type, the strain localisation is promoted mostly by kinematic hardening, is delayed by isotropic one, and the combined hardening rule occupies the intermediate position. Shear bands formation drastically distorts the finite-element mesh which eventually collapses, and thus terminates the simulation.

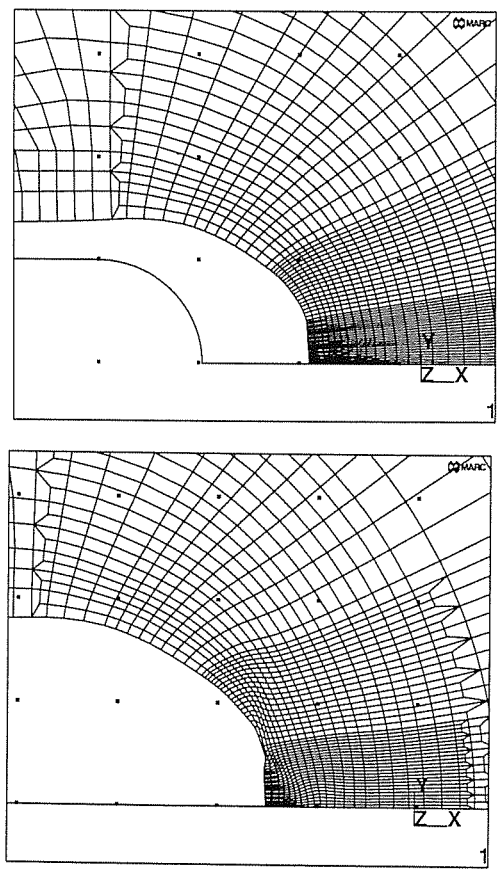

Fig. 2. Crack tip deformations at the third cycle of the loading route II with kinematic strain-hardening: (top) at the beginning of the cycle with $K = 0$; (bottom) at $K = 0.8K_{max}$ during subsequent forward load course. The grid spacing is 2.5 μm in both; the undeformed crack tip is shown in the bottom-left corner of the former one.

Analogous phenomenon of the vertex formation on the tip contour and penetration of the localised shear bands beyond the tip was found under monotonic load in the studies of the elastoplastic material with a corner (non-Mises) flow theory and isotropic power-law strain-hardening, but it was not detected when smooth (von Mises) flow rule was in use [7]. Now quite similar effect is observed with smooth von Mises yield surface under cyclic loading. It seems that plastic flow localisation is a general phenomenon, although it requires to exceed a certain level of strain, dependent on a particular constitutive model (flow and hardening rules). The evolution of strains is better displayed using the equivalent plastic strain rate $\xi_{eq}{}^{p} = d\varepsilon_{eq}{}^{p}/dt$ as a more sensitive indicator of strain localisation. This reveals that even during monotonic loading (the first forward loading phase in the simulations presented in this paper) the peak of the strain concentration, initially located at the tip apex on the symmetry axis of the crack, splits with load increase, so that two loci of plastic strain accumulation appear out of the tip apex at apparently fixed symmetric positions in respective specimen halves above and beneath the symmetry axis of the crack (Fig. 3).

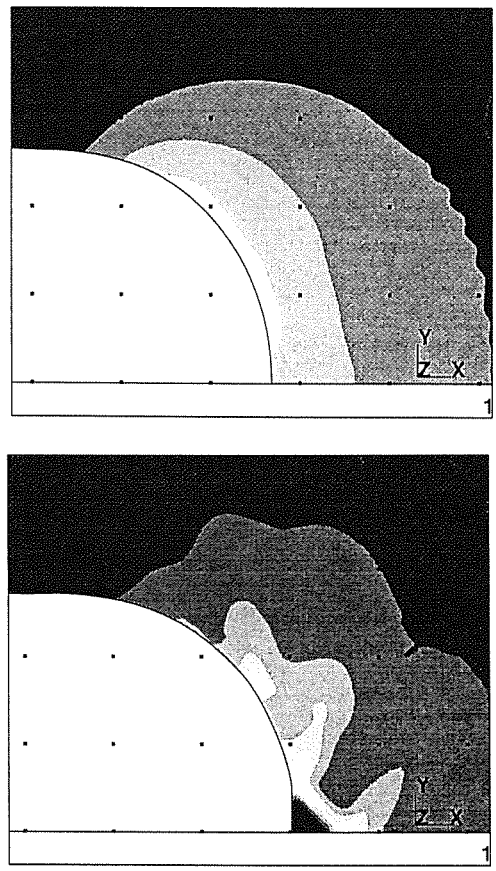

Fig. 3. Distribution of equivalent plastic strain rate near deformed crack tip when K_{max} is attained during the initial monotonic load stage of the loading regime II: (top) isotropic hardening; (bottom) kinematic hardening. Identical equidistant-section bands with $\xi_{eq}{}^{p}$ increase from dark to bright in arbitrary units; the grid spacing is 2.5 μm in both pictures.

Nucleation of these strain concentration sites out of the plane of the crack in the monotonic loading stage is common for all considered constitutive behaviours, although for each of them localisation of strain has important quantitative distinctions. Roughly, the strain concentration nuclei are more steep (more localised) and heighten faster when changing from perfect plasticity

through isotropic hardening towards kinematic one for which the strain accumulation peak becomes the most acute. Correspondingly, the efficacy of different kinds of hardening varies in the same order with regard to the rate of shear band development when loading progresses (monotonically or cyclically). At isotropic hardening these separated maxima of strain are quite round and wide, so that sufficient resolution is required to detect them, higher than that used in the previous studies of monotonically loaded crack such as [6,7]. On the other hand, sharp localisation of plasticity at kinematic hardening requires sufficient mesh refinement to reveal the effect. In general, strain localisation near the crack tip seems to be driven by increase of the (accumulated) plastic strain in every considered case, although the rate of the shear bands development depends strongly on a specific kind of hardening. To this end, not only the kind of hardening (kinematic, isotropic or other), but also the hardening rate $H = d\sigma_{eq}/d\varepsilon_{eq}^{p}$ can potentially affect the near tip localisation of strain. In particular, nonlinear constitutive behaviour with diminishing of H, such as the power-law hardening (1), is expected to favour localised shear more than linear one with H = *const.*

3.2. Near Tip Stress Fields

Only minor distinctions can be found when the stress fields in strain-hardening materials are compared with the analogous data for a perfectly plastic model [8,9]. In respective material points, stresses follow along nearly stable cyclic trajectories with no substantial dependence on the cycle number N (Fig. 4, in this paper the odd times $t = 2N - 1$ correspond to the load maxima and the even ones $t = 2N$ to the minima in the N-th cycle). The extrema of the stress alternation do not vary appreciably with K_{max}, nor they are significantly affected by the overload cycle.

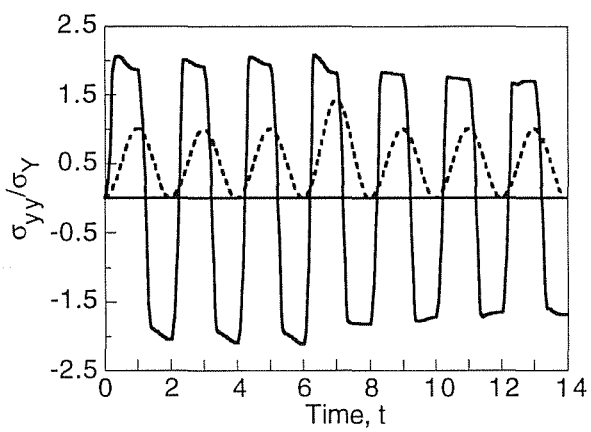

Fig. 4. Evolution of the axial stress ahead of the crack tip under sine-shape pattern of the applied loading route III with an overload peak at $t = 7$ ($N = 4$) shown by the dashed line in arbitrary units A combined isotropic-kinematic rule for strain-hardening was used in this case.

Spatial distributions of the principal stresses for all constitutive models, like the example in Fig. 5, are quite similar to the perfectly plastic case [8,9]. Some peculiarities arise only on the later stages of deformation when a slight local ridge of the normal stress may be detected associated with the shear band.

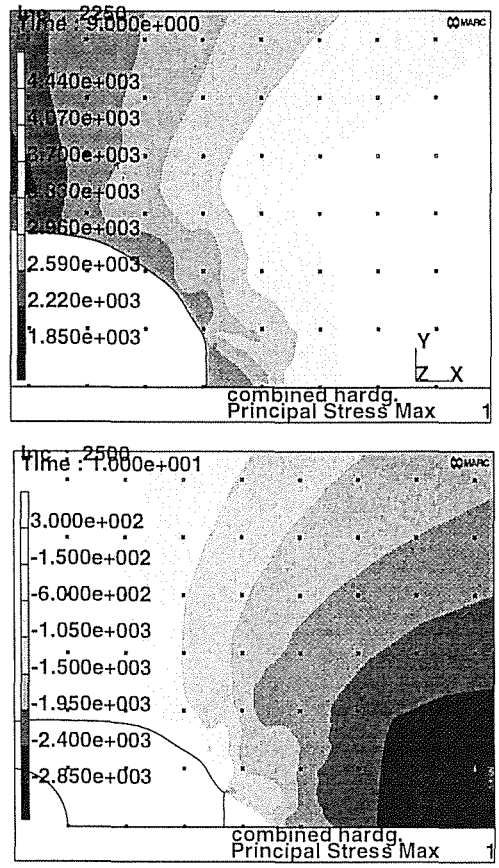

Fig. 5. Maximal principal stress (MPa) in the course of the loading regime II with combined hardening rule: (top) at $t = 9$ with $K = K_{max}$; (bottom) at $t = 10$ with $K = 0$.

3.3. Plastic Strain Accumulation

Strain-based parameters are often used as measures of damage accumulation in fatigue [13]. They are the cumulative equivalent plastic strain ε_{cum}^{p} and the total (actual) equivalent plastic strain ε_{eq}^{p} (in the case of plane-strain incompressible plasticity this represents the principal strains) which are defined along a specific path in the space of plastic strain components ε_{ij}^{p}, respectively, as follows:

$$\varepsilon_{cum}^{p} = \int\left(\tfrac{2}{3}\varepsilon_{ij}^{p}\varepsilon_{ij}^{p}\right)^{1/2}, \quad \varepsilon_{eq}^{p} = \left(\tfrac{2}{3}\int\varepsilon_{ij}^{p}\int\varepsilon_{ij}^{p}\right)^{1/2} \qquad (2)$$

Cyclic strains at considered hardening rules evolve in similar manners, the main difference being the cycle number N at which shear bands appeared. Taking the data for combined rule as an example, the main features of strain evolutions are presented in Figs. 6-8. Under

constant amplitude loading, $\varepsilon_{cum}{}^p$ increases always with fairly constant averaged rates $\varepsilon_{cum}{}^p/dN$ everywhere in the crack tip zone provided strain localisation has not started yet (curve 1 in Fig. 6). After shear bands creation, as in the load case II where localisation appears at $t \approx 6$, the increase of $\varepsilon_{cum}{}^p$ decelerates in the interior of the wedge-shaped zone between the bands, accelerates sharply within the bands, (respectively, curves 2 and 3 in Fig. 6), and maintains a fairly constant rate outside. Generally, these rates are higher for greater values of K_{max} in the course of constant amplitude cycling.

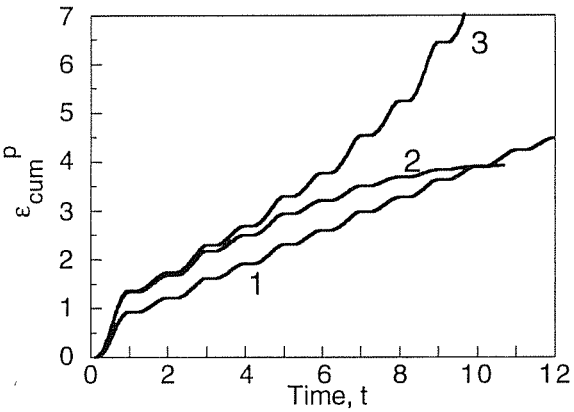

Fig. 6. Typical patterns of the cumulative plastic strain near the crack tip under constant amplitude cycling in the material points at about the same distance from the tip contour: (1) at the tip apex when shear bands do not arise, load case I; (2) and (3) respectively, in the shear band and at the tip apex belonging to the wedge-shaped zone between the bands, load case II.

A single overload, apart of a step-wise increase of the cumulative strain, has no appreciable influence on the rate of its evolution during subsequent cycling if compared with the constant amplitude regime (Fig. 7, shear bands initiate at $t \approx 10$).

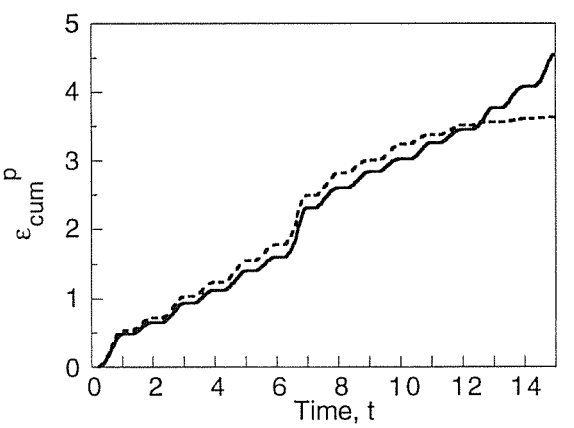

Fig. 7. Cumulative strain evolutions in the material points at about the same distance from the tip contour during fatigue with an overload peak at $t = 7$ (load case III) in the shear band (solid line) and in the wedge-shaped zone between the bands (dashed curve).

The instantaneous plastic strain value $\varepsilon_{eq}{}^p(t)$ evolves in an oscillating ratcheting manner (Fig. 8). During constant amplitude loading, the averaged (cyclic) ratcheting rate $d\varepsilon_{eq}{}^p/dN$ increases with rising of K_{max}. In contrast to the effect on the cumulative plastic strain, a single overload terminates ratcheting of the equivalent strain everywhere in the process zone.

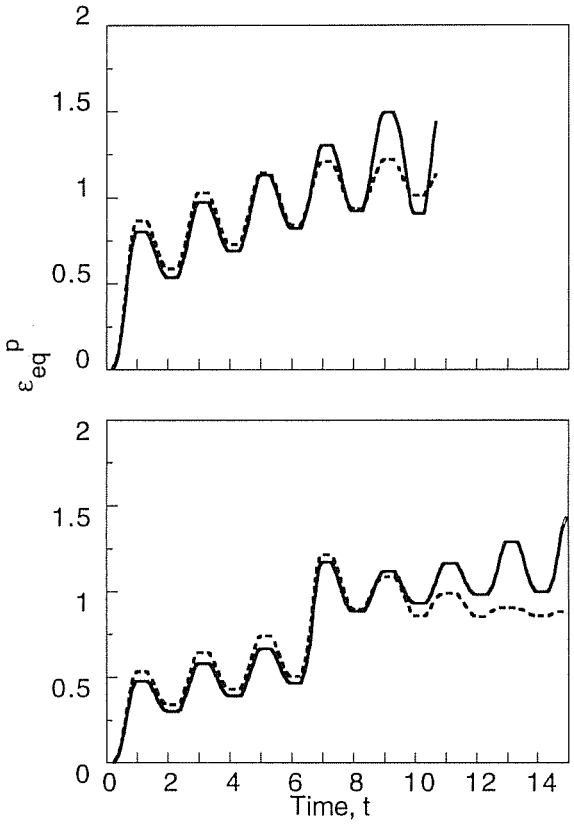

Fig. 8. Typical variations of the equivalent plastic strain near the crack tip in the material points at about the same distance from the tip contour during constant amplitude cycling (load case II, top graph) and in fatigue with an overload peak at $t = 7$ (load case III, bottom figure) in the shear band (solid lines) and in the wedge-shaped zone between the bands (dashed curves).

4. DISCUSSION

On the basis of these results, certain implications may be derived with regard to the criteria of fatigue crack growth. These criteria are usually formulated associating the local rupture event with some critical condition in terms of local stress, strain, or both them as governing factors of fatigue degradation of material. Numerical modelling shows that the stress fields in the supposed fracture process zone are nearly insensitive to the fatigue loading parameters (the amplitude K_{max} and overload level K_{ov}). In all simulated regimes, stresses oscillated between nearly equal tension-compression limits. This contrasts with rather general experimental trends of increase of the fatigue crack growth rates da/dN with K_{max} and retardation of the constant amplitude fatigue crack propagation after an overload peak [13].

In the matter of the cumulative plastic strain which supposedly controls fatigue damage accumulation [13], it manifests better correspondence with experimental data about the role of K_{max} on crack growth rates *da/dN*: both experimental crack growth and calculated strain accumulation accelerate with the load amplitude increase. However, this affinity between crack growth and cumulative strain fails with regard to the effect of an overload on fatigue.

The evolutions of the current equivalent plastic strain $\varepsilon_{eq}^{p}(t)$ reveal better parallelism with known trends of the crack growth rate variation with regard to the roles of both load amplitude and overloads. Although $\varepsilon_{eq}^{p}(t)$ oscillates, its subsequent maxima increase with cycle number in a ratcheting manner. This increase is faster at higher K_{max}, and is arrested by an overload peak (Fig. 8). Then critical strain criterion of local rupture seems to be promising to predict fatigue crack growth rates. However, to ensure better predictions, some combined critical condition may be required supposing that the limit level of the instantaneous plastic strain ε_{eq}^{p} at rupture must be a function of the two more variables: the cumulative plastic strain ε_{cum}^{p} which represents cyclic increase of material degradation, probably up to a certain maximum saturated level, and the level of tensile stress in potential rupture sites which helps material separation

Finally, formation of the shear bands implies the possibility of the Cottrell-type dislocational mechanism of microfracture being operative ahead of the crack tip at the intersection of the persistent slip planes. This indicates possible location of the nucleation of strain controlled crack-tip rupture.

5. CONCLUSION

The performed high-resolution large-deformation finite-element analysis of a stationary plane-strain tensile crack in a strain-hardening elastoplastic material under various fatigue load patterns reveals good agreement of the calculated characteristics of the plastic strain ratcheting in the near tip zone with the experimental trends of the variation of the fatigue crack growth rate depending on the applied load amplitude and overload peaks. This creates a promising basis for linking stress-strain analysis with micromechanical rupture mechanics and prediction of the fatigue crack extension.

Acknowledgements

The financial support of this research provided by CICYT (Grant MAT97-0442) and Xunta de Galicia (Grants XUGA 11801B95 and XUGA 11802B97) is gratefully acknowledged. In addition, one of the authors (VKh) is indebted to the Xunta de Galicia for supporting his stay as a visiting scientist in the Materials Science Department of the University of La Coruña.

REFERENCES

1. Blom A.F. and Holm D.K. "An experimental and numerical study of crack closure", Eng. Fracture Mech., 22, 997-1011 (1985).
2. McClung R.C. and Sehitoglu H. "On the finite element analysis of fatigue crack closure — 2. Numerical results", Eng. Fracture Mech., 33, 253-272 (1989).
3. McClung R.C., Thacker B.H. and Roy S. "Finite element visualization of fatigue crack closure in plane stress and plane strain", Int. J. Fracture, 50, 27-49 (1991).
4. Zhang X., Chan A.S.L. and Davies G.A.O. "Cyclic plasticity and overload effect on fatigue crack propagation", Computational Plasticity: Fundamentals and Applications. Pineridge Press, Swansea, 1561-1572 (1992).
5. Ellyin F. and Wu J. "Elastic-plastic analysis of a stationary crack under cyclic loading and effect of overload", Int. J. Fracture, 56, 189-208 (1992).
6. McMeeking R.M., "Finite deformation analysis of crack tip opening in elastic-plastic materials and implications for fracture", J. Mech. Phys. Solids, 25, 357–381 (1977).
7. Needleman A. and Tvergaard V. "Crack-tip stress and deformation fields in a solid with a vertex on its yield surface", Elastic-Plastic Fracture: Second Symposium. Vol. I — Inelastic Crack Analysis", ASTM STP 803. Philadelphia, 80–115 (1983).
8. Kharin V. and Toribio J. "Alternating stress-strain fields near a crack tip under cyclic loading", Anales mec. fractura, 15, 355-360 (1998).
9. Toribio J. and Kharin V. "High-resolution numerical modelling of stress-strain fields in the vicinity of a crack tip subjected to fatigue", Fracture from Defects, Proc. 12th Eur. Conf. Fracture, Vol. 2. EMAS Publishing, Warley, 1059–1064 (1998).
10. Gortemaker P.C.M., de Pater C. and Spiering R.M.E.J. "Near-crack tip finite strain analysis", Proc. 5th Int. Conf. Fracture, Pergamon Press, Oxford, 151–160 (1981).
11. Toribio J. and Kharin V. "Stress corrosion behaviour of high-strength steel: the role of fatigue pre-cracking", J. Mech. Behav. of Mater., 9, 205-225 (1998).
12. Toribio J. and Lancha A.M. "Effect of cold drawing on susceptibility to hydrogen embrittlement of prestressing steel", Mater. and Struct., 26, 30–37 (1993).
13. Suresh, S., "Fatigue of Materials", Cambridge University Press, 1991.
14. MARC User Information, Marc Analysis Research Corp., Palo Alto, 1994.